Automotive and Engine Technology (2021) 6:247–259
https://doi.org/10.1007/s41104-021-00090-5

ORIGINAL PAPER

Design and evaluation of an engine-in-the-loop environment for developing plug-in hybrid electric vehicle operating strategies at conventional test benches

Maximilian Dietrich[1] · Kunxiong Ling[1] · Roland Schmid[1] · Zhao Song[1] · Christian Beidl[2]

Received: 27 April 2021 / Accepted: 24 August 2021 / Published online: 3 September 2021

Abstract
Due to a large number of degrees of freedom and connected powertrain functionalities, the development of operating strategies for plug-in hybrid electric vehicles is an especially complex task. Besides optimizations of drivability, noise, vibrations and harshness as well as energy efficiency, the main challenge lies in ensuring emissions conformity. For this purpose, test vehicles are typically applied to achieve a realistic test and validation environment. However, operating strategy calibration using test vehicles has the drawbacks, that (i) it is very time consuming and cost intensive, (ii) it can only be conducted in late development phases and (iii) cannot be applied to reproducing driving loads for a valid comparison. To overcome these issues, this paper presents a consistent engine-in-the-loop approach combining real engine hardware and multiple software elements to represent PHEV behavior at the engine test bench. Thereby, an environment is created, which allows for realistic, flexible, cost efficient and reproducible testing. The effectiveness of the presented framework is evaluated by comparing relevant on-road measurements with their reproduction at the engine test bench. The results show that the vehicle on-road behavior can be replicated using the described testing environment. Particularly engine start/stop behavior and load levels—the core functionalities for operating strategy calibration—are matched. The proven level of realism in powertrain behavior enables further use cases beyond on-road measurement reproduction, i.e. varying individual component properties and observing real-world consequences at the test bench without the need for vehicle tests.

Keywords PHEV · Plug-in hybrid electric vehicle · Engine-in-the-loop · Test bench · Operating strategy

Abbreviations

a	Acceleration in m/s^2
B	Benefit in g/kWh
BC	Battery control
BOS	Basic operating strategy
CD	Charge depleting
C	Cost in g/kWh
CS	Charge sustaining
ECU	Engine control unit
EiL	Engine-in-the-loop
EV	Electric vehicle
HEV	Hybrid electric vehicle
HCU	Hybrid control unit
HVS	High voltage storage
ICE	Internal combustion engine
k	Time index
LPI	Load point increase
$\dot{m}$	Fuel mass flow in g/h
NEDC	New European Driving Cycle
NVH	Noise, vibration and harshness
P	Power in kW
PHEV	Plug-in hybrid electric vehicle
RDE	Real Driving Emissions
SOC	State of charge
TWC	Three way catalyst
v	Velocity in m/s
WLTC	Worldwide harmonized Light-duty Test Cycle

✉ Maximilian Dietrich
maximilian.dietrich@bmw.de

[1] BMW Group, Knorrstraße 147, 80788 Munich, Germany

[2] Institut für Verbrennungskraftmaschinen und Fahrzeugantriebe, Technische Universität Darmstadt, Otto-Berndt-Straße 2, 64287 Darmstadt, Germany

1 Introduction

In the past years, plug-in hybrid electric vehicles (PHEV) have attracted considerable attention in the search for alternatives to internal combustion engines (ICE) as means of vehicular power sources [5, 6, 8, 11, 13, 14]. PHEVs can be characterized as an intermediate concept between purely electric vehicles (EV) and conventional hybrid vehicles (HEV): Similar to HEVs and as opposed to EVs, PHEVs utilize fuel that is burned in an internal combustion engine as another source of energy than electricity stored in the battery (high-voltage storage, HVS). However, unlike HEVs and similar to EVs, a PHEV battery can be charged externally via a power outlet and the electricity grid. Combined with a larger HVS capacity than for HEVs, standalone electric propulsion for longer distances is enabled, while somewhat limited in comparison with EVs [19]. For operation exceeding the distance that can be covered electrically and for phases of high power demand, the combustion engine can be used as an alternative or additional power source.

The core instance that is responsible for the coordination of these power sources is the operating strategy. Typically, vehicle manufacturers offer a multitude of different operating modes that can be selected automatically or upon the driver's demand. The most widespread types are charge depleting (CD) and charge sustaining (CS) mode: In CD mode, the PHEV is mainly powered electrically with the combustion engine providing assistive power if needed, which leads to decreasing HVS state of charge (SOC). In this case, brake energy recuperation is the only source of electricity for recharging the battery while the vehicle is operated. In CS mode, the battery SOC is kept roughly constant, which is achieved by more frequent and prolonged ICE operation substituting electric operation [19]. Additionally, the SOC can be actively raised by the ICE providing more power than needed for vehicle propulsion and the electric motor operating as a generator (battery control, BC). More advanced control strategies can, for example, include predictions of energy demand along the driven route [4, 9].

The multitude of operating states resulting from those modes contributes to a significant increase in development efforts compared with conventional vehicles, while development time frames are at the same time continuously tightened. Careful adjustments of complex control functions, commonly referred to as calibration, have to be undertaken to simultaneously achieve conflicting targets like maximum energy efficiency, drivability and comfort levels, especially concerning noise, vibration and harshness (NVH). Additionally, effective measures have to be taken to ensure compliance with pollutant emission limits within the vehicle type approval process. This especially complex task is called emissions calibration and is the main driver behind this work. It covers tuning of all emissions relevant engine control function parameters, particularly those responsible for catalyst heating, engine start and after-start behavior as well as lambda, i.e. air–fuel ratio, control. Using the fuel consumption criterion as an example, a conflict of interest typically encountered during emissions calibration can be illustrated in more detail: To achieve minimal fuel consumption, the ICE should be switched off for as long as possible. During those phases of ICE inactivity, exhaust gas aftertreatment systems like three-way catalysts (TWC), which require certain temperature levels for effective operation, can cool down, leading to elevated tailpipe emission levels in the beginning of subsequent phases of active ICE operation [18] While this phenomenon typically occurs only once at the start of the trip for conventional ICE-powered vehicles, the PHEV operating strategy can lead to several of these "cold start" events in a single trip, separated by phases of electrically powered driving. Additionally, ICE assistance is usually required in phases of high power demand, leading to ICE operating points favoring high raw emissions and therefore intensifying the described emissions problem even further [12].

On top of the technical challenges of PHEV emissions calibration, new legislative boundary conditions require even more attention and effort: While standardized driving cycles like the New European Driving Cycle (NEDC) [1] nd Worldwide harmonized Light-duty Test Cycle (WLTC) [21] have long been the reference for emission measurement during certification and, therefore, also for powertrain design and calibration, the recent legislative overhaul in the European Union in the form of the introduction of Real Driving Emissions (RDE) [2] shifts the focus towards more diverse and customer-centric driving profiles. Consequently, previously used criteria for the development of PHEV operating strategies that were relying on fixed driving profiles, e.g. the WLTC as a basis for the determination of fuel consumption, may now lead to adverse tailpipe pollutant emissions results in a randomized RDE test.

As a development environment for efficient and effective operating strategy emissions calibration, on-road vehicle tests are not optimal but are currently used nevertheless due to a lack of alternatives. While all necessary influences are present by nature of the test, insufficient reproducibility, high costs for measurement time and generally late vehicle availability in the development process favor different approaches [15]. Existing chassis dynamometers offer only a partial solution: While testing conditions are reproducibly controllable and the use of a complete vehicle as the test subject ensures realistic test results, the issues of vehicle availability and high costs for manual test execution remain. Engine test benches, as they are used for the calibration of conventional powertrains, can offer ways to overcome said shortcomings. However, they need to be extended to allow

for realistic operating strategy behavior without the presence of the real vehicle and the multitude of sensors, actuators and control units that entails. Coupling real powertrain hardware with simulated components, engine-in-the-loop (EiL) test beds are particularly well-suited for emissions investigations at early development stages [3]. The availability of a real engine as the main testing subject enables accurate emissions measurements and analyses. Simultaneously, additional simulation elements can provide realistic inputs from, for example, driver, vehicle or environmental models. With real and simulated parts continuously influencing and reacting to each other, the information flow loop is closed.

Within this work, a simulation framework is introduced, which consists of models of the electric motor, the HVS and the operating strategy itself. The framework intends to supplement the real ICE hardware on the conventional engine test bench, enabling cost-efficient and reproducible, yet realistic PHEV operating strategy investigations for emissions calibration purposes.

The paper is structured as follows: A description of the proposed testing framework and its individual elements is given in Sect. 2. Section 3 presents and discusses the results that were obtained from a comparison between vehicle and test-bed measurements. These serve as proof of concept for the developed EiL environment and its ability to correctly reflect real-world powertrain behavior. On this basis, tests involving parameter changes within the operating strategy or other powertrain components can be conducted at the test bench, exceeding the use case of pure on-road measurement reproduction. This enables far-reaching elimination of vehicle tests altogether. As an example, the effects of modified torque demand thresholds for ICE start up are detailed in Sect. 4. Finally, Sect. 5 contains a summary of the procedure, the conclusions that could be drawn and possible future extensions of this work.

2 Framework

For recreating real-world PHEV driving scenarios at the engine test bench, an interconnected framework covering all relevant functionalities has been created. It can generally be divided into a hardware domain consisting of the engine and the test bench equipment, as well as a software domain. For the latter, a modular approach based on individual simulations of the electric motor, the high voltage storage and a simplified representation of the operating strategy was chosen within this work, enabling easy interchangeability of individual components. Hereafter, each of these models, which were created in MATLAB/Simulink and integrated into the test-bed automation system, is described in more detail.

As a first step towards shifting test efforts from vehicles to the proposed EiL test bench environment, the individual model reproduction quality is assessed. For this purpose, the respective inputs are supplied directly from on-road measurements. Thereby, testing framework component behavior can be validated in a direct comparison before more advanced tests of the complete framework are performed (see Sect. 3).

As a basis for model validation, on-road measurements have been conducted with a BMW 330e test vehicle. All relevant hardware components at the test bench as well as simulation model parameters that are used in this work and reflect vehicle-specific properties match this reference vehicle. For each model, affected parameters are described in more detail below.

To evaluate the agreement between simulated and measured PHEV operations, a 65-min long test drive was conducted. It resembles real-world driving behavior with varying traffic conditions and features a wide range of operating conditions during phases of urban, rural and motorway driving as well as a transition from CD to CS operation. Thereby, it contains all relevant aspects for emissions calibration under RDE boundary conditions. Figure 1 shows the measured trajectories of throttle amplitude, vehicle velocity as

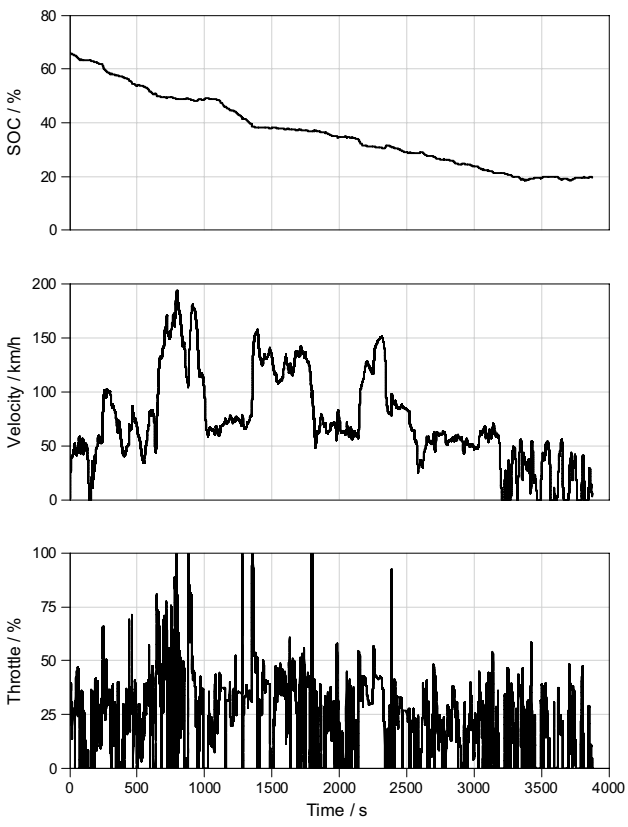

Fig. 1 Throttle, velocity and SOC trajectories of the on-road test drive

well as SOC. All reference measurement data used for validation and in the corresponding figures have been recorded during this driving scenario.

2.1 Test bench setup

The testing hardware is representative of a typical conventional dynamic engine test bench at the BMW Group test facilities. It is equipped with a Siemens load unit supporting engine torque values of up to 400 Nm and speeds of up to 10,150 1/min and therefore enables realistic ICE operation under all conditions. For ICE start-up, shutdown and idling, a pneumatically operated clutch is used to separate the load unit and the engine. The test subject is a four-cylinder gasoline engine of the same type as in the reference vehicle. All testing equipment is controlled and monitored through the automation system (FEV Morphee), which also runs additional simulations of, for example, the automatic gearbox. Direct access for measuring functions and values within the engine control unit (ECU) is given through the calibration system (ETAS INCA), with a complex custom residual bus simulation providing all necessary inputs for realistic engine behavior.

2.2 Electric motor model

For this work, the most important characteristic of the electric motor is its power demand, which results from the operating point defined by torque and speed and leads to battery discharge or charge. As a simplified modelling approach, we have chosen to use a two-dimensional look-up table containing measured data of electric currents over electric motor torque and speed (see Fig. 2). The necessary data are extracted from existing component validation measurements of the electric motor used in the reference vehicle mentioned above that are performed at component test benches at a constant operating voltage of 320 V. Within the chosen speed intervals of 500 1/min, a linear correlation between the electric current and motor speed and torque, respectively, can be assumed. For electric current determination, linear interpolation between the measured data points stored in a Simulink look-up table can therefore be used for accurate data selection with low computational demand. The model yields reasonably good agreement when simulated electric currents are compared with real driving measurements (see Fig. 3). The qualitative signal behavior is replicated accurately with a minor systematic underestimation of the measured values by the model, the effects of which are discussed in Sect. 3. Combined with the ease of parametrization and low computational demand, this makes for an attractive method for simulating electric current drawn or provided by the electric motor.

2.3 High-voltage storage model

The electric motor current causes the battery to be discharged or charged, thereby affecting SOC, which is simulated by the HVS model. It is based on an existing in-house development and represented by an equivalent circuit model consisting of resistors (R) and capacitors (C) that are connected as depicted in Fig. 4. Since this structure is commonly found in many battery models and widely discussed in literature, we direct the reader towards such sources for in-depth descriptions [7, 10, 22–24]. Within the work at hand, this model was parameterized using BMW Group internal data for U_0 (SOC-dependent curve), the resistances of R_1, R_2, R_3 (mapped over SOC and electric current) as well as the capacities of C_2 and C_3 (mapped over SOC and electric current) to represent the reference vehicle HVS. These data are provided by the respective BMW Group department. They are based on battery cell measurements using stepwise discharging and charging for open-circuit voltage determination as well as dynamic current pulses (current interruption technique) to determine resistance and capacity values [7]. While the data are available for different HVS temperature

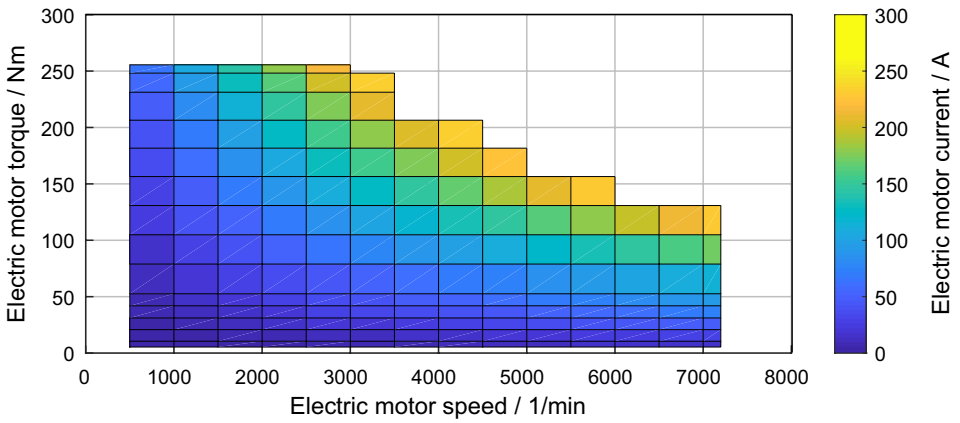

Fig. 2 Mapped data for the electric motor model

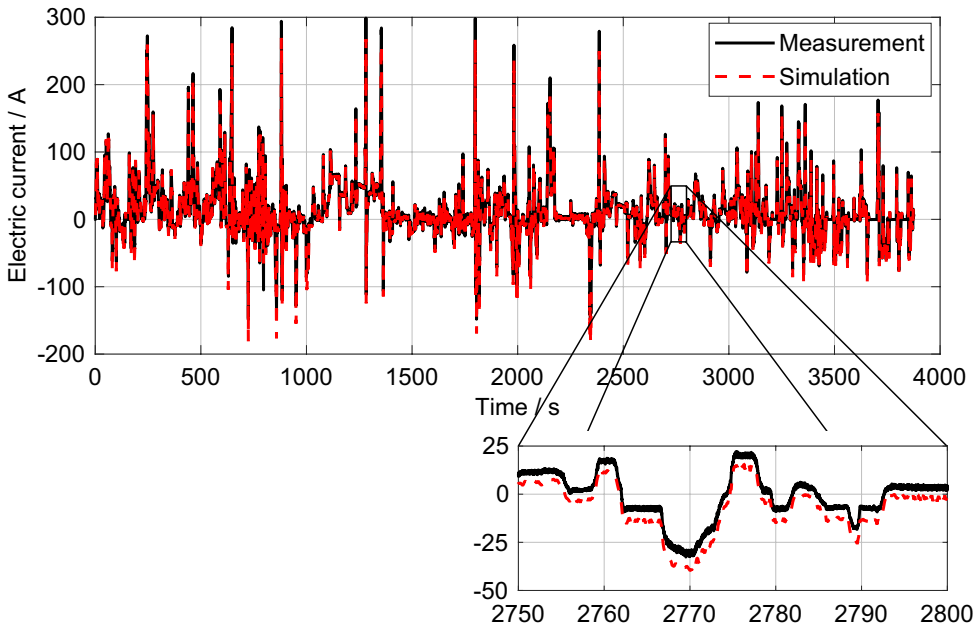

Fig. 3 Comparison between measured and simulated electric currents drawn by the electric motor

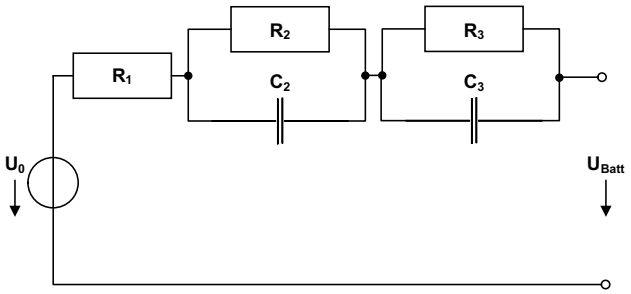

Fig. 4 Equivalent circuit model for HVS model; U_0 open-circuit voltage, U_{Batt} battery voltage

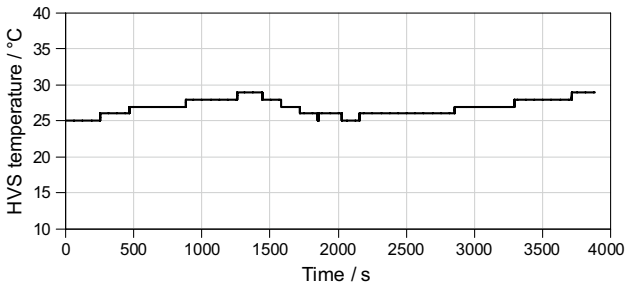

Fig. 5 HVS temperature as measured during a dynamic on-road driving scenario

levels of 0 °C, 25 °C and 40 °C, the HVS temperature is regarded as a constant value of 25 °C within this work to reduce storage space and simplify parameter handling. As Fig. 5 shows, this is a justified assumption since the vehicle battery cooling/warming system is working ideally under normal conditions and is able to maintain HVS temperatures

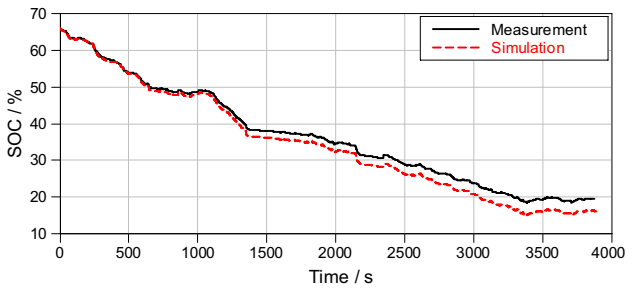

Fig. 6 Comparison between measured and simulated SOC using the measured electric current as input

between 25 and 29 °C during the recorded dynamic driving scenario (see Fig. 1 for additional information).

Figure 6 shows a comparison of simulated and measured SOC trajectories during a dynamic real-world trip and gives an indication of the HVS model performance. For this evaluation, the model was directly fed with the current from the electric motor as it was measured on the road. As the comparison shows, the model is able to simulate the real SOC trajectory qualitatively. An almost linearly increasing quantitative deviation can be observed, accumulating to about 3.5% SOC at the end of the simulation. This modelling error is assumed to be a consequence of both the simplified model structure and the chosen temperature-independent parameterization. Comparing Figs. 5 and 6, it can be noted that deviations of SOC gradients are more apparent whenever the actual HVS temperature is notably higher than the modelled constant state of 25 °C, which supports this assumption. These results show that particular attention needs to be given to possible effects of different SOC values

regarding powertrain behavior that might occur during a direct comparison between vehicle and on-road tests within the complete testing environment (see Sect. 3). However, the observed SOC deviation can be regarded as a systematically occurring error, which is always present when this model is used. Repeated SOC modelling yields identical results with the same SOC trajectory, enabling reproducible tests. For test-bed exclusive tests without a vehicle reference, adverse influences affecting reproducibility are therefore not to be expected.

2.4 Operating strategy model

As the core instance for determining ICE and electric motor operation mode as well as torque distribution and energy management, the operating strategy plays a fundamental role in realistic powertrain behavior at the test bed. A full replication of the respective functions running on the vehicle hybrid control unit (HCU) in the test-bed environment would require additional simulations of a multitude of signals and input data, which are not easily available, or additional hardware to power the physical HCU, leading to considerable development effort and investments. For the task at hand, it was therefore decided to use a reduced model of the basic operating strategy (BOS), which, unlike more advanced operating modes, does not depend on predictions of the driven route, for example, but contains only the most important functions for the determination of ICE start triggers and torque split between the ICE and electric motor. The model implementation, including SOC mode recognition, E-drive decision, SOC control and power split described below, has been adopted from previous work [20]. Additional effort went into creating suitable interfaces for connecting to the previously described electric motor and HVS models. Other model components such as component thermal behavior and mechanical endurance estimation that originate from the cited work have been removed as they are not needed for the intended application described here.

Specifically, the resulting model covers the following operating strategy functionalities:

- Automatic transition from CD to CS operation based on SOC.
- BC operation based on user request.
- Triggering ICE start and shutdown based on driver power demand, road inclination, driving velocity, driver acceleration demand as well as drivability and NVH restrictions (e.g. avoiding repeatedly starting the ICE within a certain time window).
- ICE load point shifting for HVS charging or more efficient overall operation.
- Short-term electric boost to support ICE operation.
- Brake energy recuperation.
- Drive mode (e.g. comfort, sport, electric) dependence of the points mentioned above.

Figure 7 illustrates how the criteria listed above are handled within the BOS model: All decisions are based on the driver's commands, i.e. the chosen powertrain modes and torque demand, as well as the current powertrain state and operating point.

As the top-level influence, these inputs determine whether CD or CS operation is active. In the respective mode, the decision about purely electric propulsion (e-drive) is based on a comparison of the driver's acceleration request with pre-defined acceleration-velocity (a–v) curves as they are

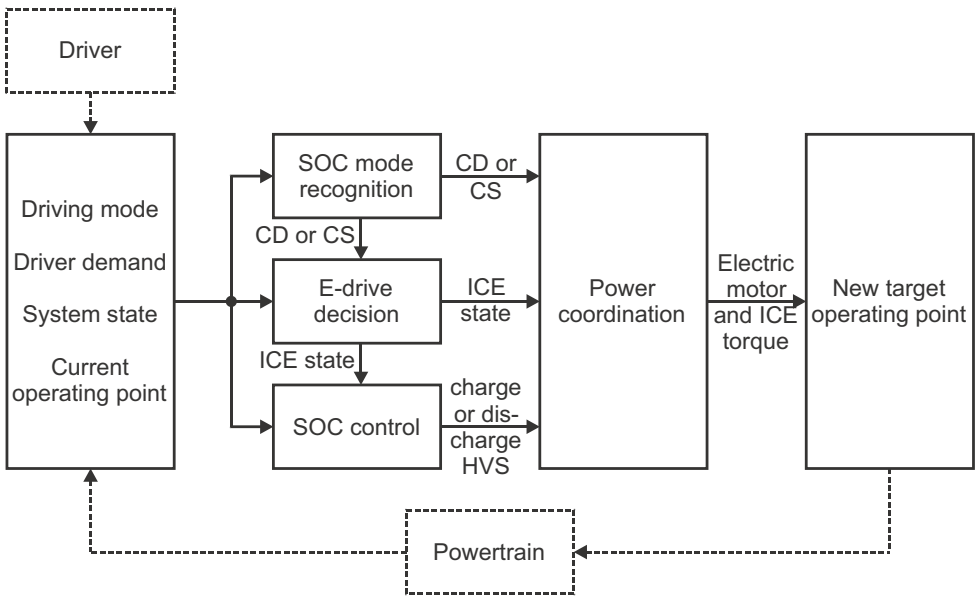

Fig. 7 Structure of the operating strategy model (adapted from [20])

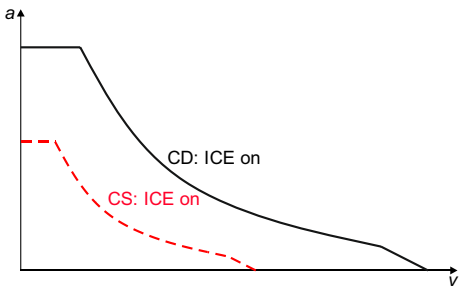

Fig. 8 Schematic *a*–*v* curves for CD and CS mode

implemented in real vehicle HCU functions. As shown schematically in Fig. 8, the ICE needs to operate whenever the current *a*–*v* values exceed the limits defined by the curves. While the vehicle can be driven electrically at higher velocities in CD mode, the velocity range is reduced in CS mode to limit electric motor torque output and thereby SOC consumption.

From the overall power demand and the determined ICE state, the final decision regarding the power split between electric motor and ICE is made to achieve optimally efficient SOC control. As soon as SOC reaches a lower boundary of the optimal working range, HVS charging is activated to raise the battery energy reserve. The required charging power is generated by requesting additional ICE torque (load point increase, LPI). If, on the other hand, the SOC exceeds an upper boundary, the recuperation function is suppressed to avoid battery overcharging and the requested ICE torque can be reduced (load point reduction, LPR) to favor consumption of the energy stored in the battery. In addition to the current SOC level, activation and power values for LPI and LPR depend on the overall operating state of the vehicle, especially with regards to fuel consumption. Following the approach introduced in [17], SOC control is realized by evaluating the cost and future benefit of a load point shift. At each time step k, the cost of LPI $C_{\mathrm{LPI}}(k)$ is defined as the extra fuel consumption caused by generating additional battery energy, and is mathematically expressed as

$$C_{\mathrm{LPI}}(k) = \left| \frac{\dot{m}_{\mathrm{LPI}}(k) - \dot{m}_{\mathrm{bas}}(k)}{P_{\mathrm{HVS}}(k)} \right|,$$

where $\dot{m}_{\mathrm{LPI}}(k)$ and $\dot{m}_{\mathrm{bas}}(k)$ are the fuel mass flow with and without LPI respectively, and $P_{\mathrm{HVS}}(k)$ denotes the battery power. As described in [17], the predicted $C_{\mathrm{LPI}}(k)$ is compared with the maximum allowed cost $C_{\mathrm{max}}(k)$, which depends on the current SOC level, and LPI is executed if

$$C_{\mathrm{LPI}}(k) < C_{\mathrm{max}}(k).$$

The lower the SOC(k) value is, the higher the tolerance for extra fuel consumption becomes. Consequently, the value of $C_{\mathrm{max}}(k)$ is raised with decreasing SOC. Similarly, the benefit of LPR $B_{\mathrm{LPR}}(k)$ is defined as the reduction in fuel consumption due to torque assistance from the electric motor:

$$B_{\mathrm{LPR}}(k) = \left| \frac{\dot{m}_{\mathrm{LPR}}(k) - \dot{m}_{\mathrm{bas}}(k)}{P_{\mathrm{HVS}}(k)} \right|,$$

with $\dot{m}_{\mathrm{LPR}}(k)$ representing the fuel mass flow after LPR. LPR is then executed if

$$B_{\mathrm{LPR}}(k) \geq B_{\mathrm{min}}(k).$$

Likewise, $B_{\mathrm{min}}(k)$ denotes the minimum required benefit for LPR and decreases with increasing SOC(k). For the respective operating point at each time step, the required fuel mass flow data for the calculations of cost and benefit are taken from fuel consumption maps. These are based on existing test-bed fuel consumption measurements for the respective ICE and stored within the model in map-based form. If the BC mode is active, the cost of LPI is neglected and any ICE power reserve for battery charging is used to raise the HVS SOC to the desired level.

Using the decisions made by the instances described above regarding CD or CS operation, active or inactive ICE and HVS charging or discharging, the driver's power demand as well as possible additional power requirements, e.g. for LPI, are distributed between the electric motor and the ICE. The following considerations influence the decision making:

- If the ICE is running, maximum available ICE power for the current ICE speed is read from a look-up table based on ICE test-bed measurements. Consequently, this value is set to zero for inactive ICE operation.
- If the driver expresses positive power demand through throttle input and the ICE is running, this demand is solely fulfilled by the ICE. In case of driver power demand exceeding maximum ICE power, the electric motor can supply additional boost power for a limited time. As is the case for real HCU functions, maximum boost power depends on the selected driving mode.
- If LPI is requested, ICE power is raised and electric motor power is reduced towards negative values, i.e. recuperation. For LPR, electric motor power is raised to reduce ICE load accordingly.

Both ICE and electric motor power demand result in new target operating points that are transmitted to the respective control units, thereby closing the control loop.

For application within this work, all relevant model parameters have been adapted to match the chosen reference vehicle and its operating strategy. In particular, this concerns SOC curves for CD/CS switching, *a*–*v* curves for e-drive decision-making, and fuel consumption maps as well

as C_{max} and B_{LPR} curves for LPI and LPR determination. These data have been supplied by the BMW Group department responsible for PHEV operating strategy development. Additionally, basic vehicle information like vehicle mass or powertrain power data was taken from internal vehicle datasheets.

The principal functionality of the BOS model and its ability to correctly determine operating modes and power split are validated in the original source [20]. Unlike the newly applied electric motor and HVS model, we have deemed additional separate BOS model validation as not required within this work, since modifications that might cause deviating behavior are restricted to the aforementioned parameter changes. Instead, we will focus on validating the combined framework and the interaction of all models at a later stage (see Sect. 3). Any mismatching BOS model behavior would become apparent there.

2.5 Combination of hardware and simulation

With the electric motor, the battery and the operating strategy existing as individual models, the core PHEV functionalities that are relevant for emissions calibration, i.e. decisions about ICE start and load levels, can be simulated using a combination of these elements in addition to operating real ICE hardware at the test bench. The complete setup is depicted in Fig. 9. For the simulation validation measurements, the signal flow is as follows: With a frequency of 10 Hz, the throttle values that were recorded during the test drive are sent to the ECU via the test-bed automation system. Similarly, the recorded rotational speed of the electric motor, which equals that of the ICE in phases of active ICE operation, is sent to the electric motor model as well as the load unit speed controller. Additionally, on-road measured vehicle speed (v) is fed into the operating strategy model. As in the real vehicle, the throttle signal is interpreted by the ECU, transformed into driver torque demand and sent to the operating strategy for further evaluation. Based on the various criteria listed above, the operating strategy determines the torque split between electric motor and ICE and whether the ICE should be running. In case an ICE start is required, the respective signal is sent to the ECU via the residual bus simulation. During the startup, engine speed is monitored and once matching speed between ICE and test bench load

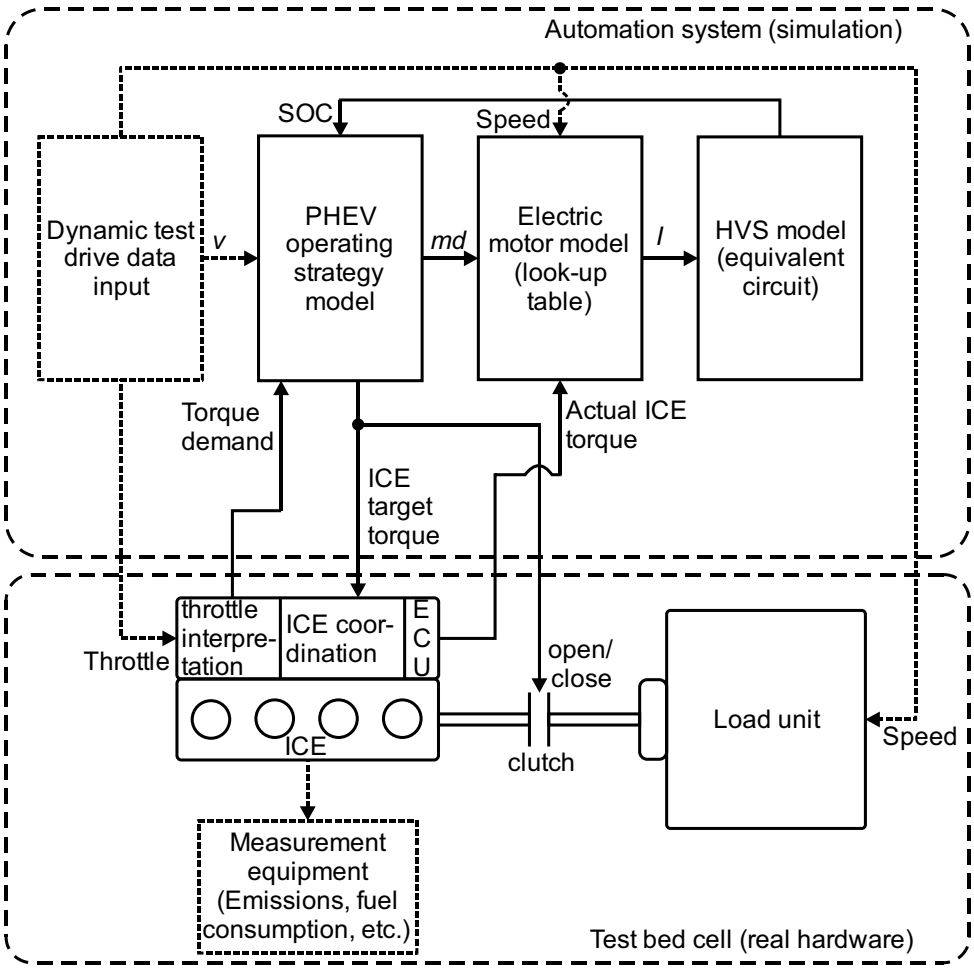

Fig. 9 Testing framework overview

unit has been reached, the clutch is closed, the engine operates normally and measurements of, for example, emissions and fuel consumption can be made. Actual ICE torque is fed back into the electric motor model alongside the torque demand from the BOS (md) so that any deviations between requested and delivered ICE torque can be compensated by the electric motor. The resulting electric current (I) is used in the battery model to determine the current SOC, which is in turn used by the operating strategy for its decision-making.

3 Framework validation

Using the setup described above, a comparison between a recorded test drive and its replication at the test bench has been made regarding ICE and electric motor torque as well as SOC progression. As opposed to the previously discussed individual modelling results, this investigation is intended to serve as proof of correct functionality of the complete framework and its ability to accurately reflect real-world PHEV powertrain behavior, which is the prerequisite for fully vehicle-independent testing at the test bench. Only throttle and velocity information from the on-road test are used, with all remaining signals being determined online at the test bed. The obtained results are described and analyzed in this section.

Plots depicting comparisons of on-road and test-bed measurements contain a note regarding typical variation ranges, i.e. the difference between maximum and minimum value, of the depicted signals as observed during tenfold repeated test execution. It is intended to serve as an indicator of measurement reliability and is given as textual information to maintain overall plot clarity.

3.1 ICE torque comparison

Comparisons between ICE torque measurements on the road and at the test bench show generally close agreement. As one example of a driving phase with active ICE operation, Fig. 10 shows a roughly 6 min long excerpt taken from on-road and test-bed measurements with an ICE start occurring at the 2173 s mark. It includes the most challenging aspects of ICE operation, which are ICE start, transient operation, as well as shut down. In this particular case, ICE start is triggered by high torque demand during an acceleration maneuver and occurs at the same time in both on-road and test bench measurement. The simulated simplified operating strategy is therefore indeed able to correctly reflect the behavior of its real-world counterpart in the vehicle. ICE torque also closely matches the values from the test drive with only minor deviations being visible during the highly transient ICE

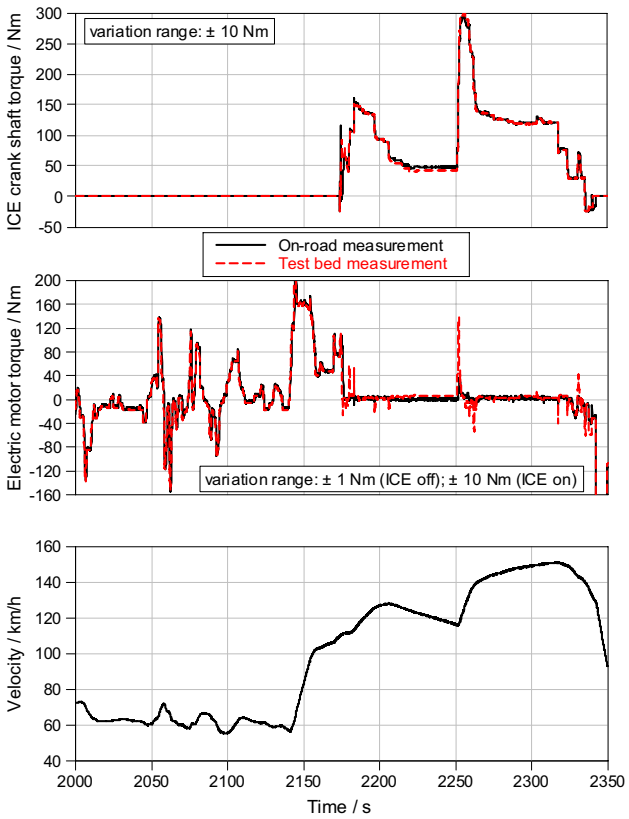

Fig. 10 Comparison between ICE crank shaft as well as electric motor torque during an excerpt of on-road and test-bed measurement

ramp-up and shut-off as well as occasionally in almost stationary operation (2205–2250 s). Given the reproduction error for ICE torque that can typically be expected for the throttle and ICE speed based control mode used at the test bench and acknowledging non-identical environmental conditions (temperature, air pressure, humidity, etc.) between on-road and test-bed measurements, these differences can be considered normal and not inherent to the applied engine-in-the-loop methodology. This assessment is based on the authors' experience with similar tests using the same control types but without the simulation framework introduced here. Furthermore, only a minor increase in reproduction quality has been observed with the methodology applied in [16] of directly using recorded torque values instead of throttle inputs and thereby bypassing the ECU torque coordination logic. Considering the comparatively small accuracy gain and the fact that using prerecorded torque values counteracts the intended execution of vehicle-independent tests, the observed accuracy is deemed sufficient. Both the torque demand that is determined by the operating strategy model and sent to the ECU as well as the resulting delivered ICE torque can therefore be considered to agree well with the reference values, signifying correct operation of the related functions.

3.2 Electric motor torque comparison

Figure 10 also shows measured and simulated electric motor torque during the same period of both inactive and active ICE operation that is discussed above. During the period with ICE standstill at the beginning of the depicted excerpt, nearly exact agreement between on-road and test-bed electric motor torque measurements can be observed. This confirms correct operation and interaction between the ECU determining overall torque demand and the operating strategy routing it towards the electric motor as intended. Since the demanded torque is almost completely delivered by the ICE while it is active, the electric motor torque fluctuates around zero, except for short moments of support operation during transient maneuvers with high torque gradients and the already observed phase of deviating ICE torque during quasi-stationary operation. These interdependencies prove the correct functionality of the connection between measured ICE torque, overall driver torque demand and modelled electric motor torque.

3.3 SOC comparison

As previously discussed during electric motor and HVS model validation, good agreement between simulated and measured electric current, resulting from the delivered torque, as well as state of charge, resulting from this current, can be expected (see Figs. 3 and 6). Given the representation of electric motor torque that has been described before, consequentially, a comparison between the measured and simulated SOC trajectories reveals close agreement (see Fig. 11). In fact, the SOC values recorded during the test-bed measurement show better agreement with the on-road measurement than during HVS model validation (see Fig. 6). In the test-bed measurement, the slightly faster SOC decay, that had been previously observed when the HVS model was fed with the measured electric current, is effectively countered by the marginally lower electric currents provided by the electric motor model (see Fig. 3). The observed effect of these systematic errors cancelling each other out does not necessarily occur when driving cycles with different conditions during on-road measurement data acquisition are used than in the shown example. Since the assumed causes for the observed deviations during individual HVS and electric motor model validation, respectively, are of differing nature, similar behavior of both effects effectively cancelling each other out cannot be expected under all possible circumstances. For example, different HVS temperatures closer to 25 °C during the measured on-road test drive would have led to faster measured SOC decay as modelled by the HVS model. However, electric motor torque would not necessarily have been influenced by these temperature changes and would therefore lead to the same resulting SOC trajectory in the test-bed measurement as pictured in Fig. 11. Under these conditions, similarly close agreement as shown in Fig. 11 would not have occurred, thus inferring the given conclusion. However, when exclusively comparing repeated test-bed measurements of the same driving cycle, reproduction quality, expressed by the shown variation range, remains unharmed.

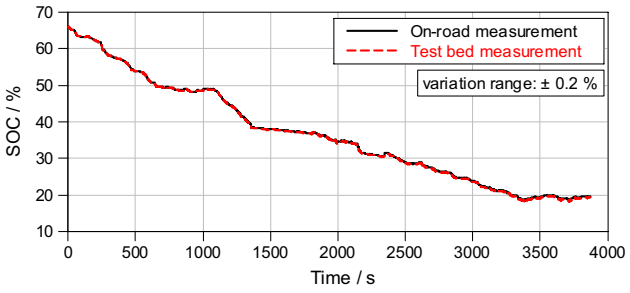

Fig. 11 Comparison between SOC during on-road and test-bed measurements

3.4 Conclusions

Overall, the obtained test-bed results can be regarded as an accurate representation of the vehicle on-road behavior despite the various simplifications that were made in the models. The testing framework ability to reproduce the measured vehicle on-road behavior is therefore confirmed. This guarantees both reliability and interchangeability of on-road and test-bed measurements and thereby lays the grounds for vehicle-independent testing at the test bench.

4 Vehicle-independent parameter variations

As described in the introduction, the main benefit of creating a test bench testing environment for PHEVs is not only the accurate reproduction of previously recorded vehicle measurements, but also the ability to conduct experiments with dedicated parameter variations under otherwise constant boundary conditions. With the proof of vehicle-like powertrain behavior having been delivered above, effects of these variations at the test bed can be expected to manifest in vehicle tests under similar circumstances. This de-facto reversal of the development flow during testing effectively contributes to the targeted frontloading with a reduced use of prototype vehicles.

To illustrate the possibilities the proposed methodology offers, parameters within the operating strategy model have been modified to investigate their effects on powertrain behavior. As an example, the torque demand threshold for triggering ICE start has been slightly raised, which

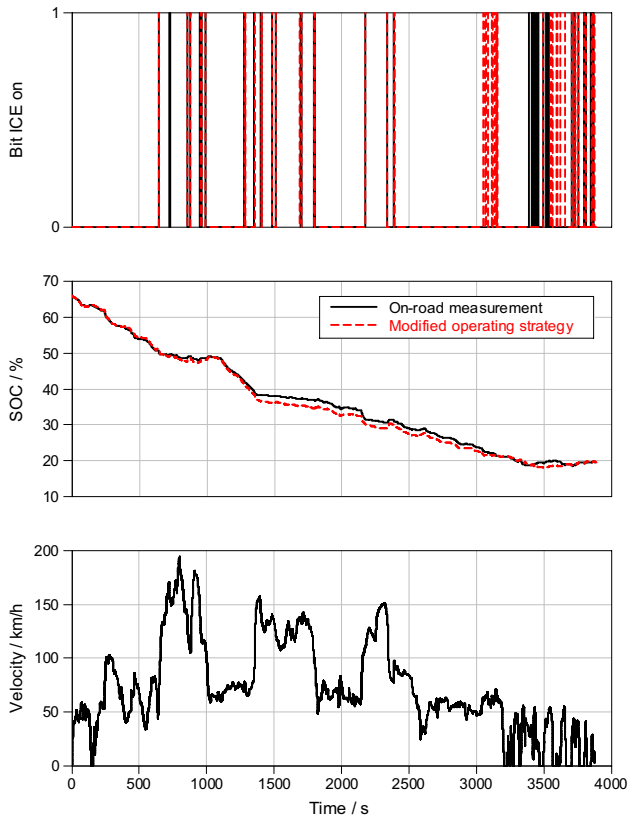

Fig. 12 Consequences of raised threshold for ICE torque support

should lead to more electric motor reliant operation. Figure 12 shows some of the effects: Up to 1350 s, no major differences between the measurements with the original and modified operating strategies can be observed. At this point, however, a sudden drop in modelled SOC can be noticed in the test with the modified operating strategy, leading to a constant SOC shift of −2% from there on in relation to the original values. As the root cause, a slightly delayed ICE start request triggered by the modified operating strategy can be identified: because the torque demand threshold has been raised, the delayed ICE start requires the electric motor to supply the driver's torque demand for longer. Since a motorway acceleration occurred in the on-road measurements at this time stamp, torque demand is high, which in turn leads to high electric motor currents and rapid HVS discharge.

These SOC deviations cause an additional effect towards the end of the measurement: At 3050 s in the measurement with the modified operating strategy, its mode changes from CD to CS. This is a direct reaction to the lower SOC level and causes repeated ICE starts to maintain battery charge. In the original measurements, this transition occurred at 3388 s. Inevitably, ICE start and stop triggers are not aligned between original and modified operating strategy measurements up to 3700 s, where SOC agreement has been restored. Again, this serves as an example of correct interaction between the modeled and physical components, with this EiL characteristic enabling use cases beyond pure reproduction of previously recorded measurements.

Combined with the chosen structure of the framework with its flexible approach for rapid interchangeability of differently parameterized individual simulated components, quick modifications within the operating strategy, and simple conversion between conventional and PHEV powertrain testing environments for optimal measurement time use, the presented methodology offers a promising basis for complete independence of vehicle measurements. For the discussed application in emissions calibration, the EiL framework that is introduced here, therefore, offers suitable performance at low costs and setup effort and can effectively aid in tackling increasing development efforts.

5 Summary and outlook

For effective holistic emissions calibration as it is required to meet the exhaust emissions limits defined by the new RDE legislation, PHEV powertrain behavior needs to be accurately replicated within a test-bed environment. Simultaneously, development time and budget restrictions are tightened, demanding efficient use of existing infrastructure without further considerable investments.

As a possible response to these challenges, methodological approaches for virtual representation of PHEV core elements at a conventional engine test bench are introduced within this work. The required simulation chain consists of models of the vehicle high-voltage storage, the electric motor as well as a simplified version of the operating strategy. This way, an EiL platform is created that does not require any additional hardware and therefore offers both flexibility as well as cost efficiency. Measurements conducted on the road and within the described test bench environment show that decisions about combustion engine start and load levels—the core operating strategy functionalities—can be realistically reproduced at the test bench. The resulting simulated electric motor torque, current and the battery state of charge are shown to be in good agreement with the measured real-world values. Interdependencies between the individual components are reflected in a realistic manner, enabling efficient vehicle-independent testing at the engine test bed.

All in all, the EiL setup offers a modular, flexible, cost-efficient, yet accurate testing environment for analyzing and optimizing a PHEV powertrain emissions behavior at early development stages. As a future project, the described simulation framework could be integrated even deeper into the test-bed automation system road load simulation. This would enable complete independence of existing vehicle measurements since throttle and braking actuation would

automatically result in adequate acceleration and in turn driving velocity values through online driving resistance calculation. The need for previously recorded velocity trajectories would thereby be eliminated.

As a competing approach, using physical representations of control units and powertrain components, which have been simulated within the scope of this work, could possibly lead to even more accurate agreement between test bench and real-world measurements. However, this would entail a much more complex framework for accurate signal flow requiring significantly higher efforts as well as additional investment in test-bed hardware.

Author contributions All authors contributed to the study conception and design. The concept for the simulation framework was developed by MD and RS. Design and parametrization of the electrical motor model were conducted by RS. The basic operating strategy model was developed by ZS and KL. Parametrization for the used vehicle was performed by MD, KL and ZS. On-road measurements as well as model integration into the test-bed environment were conducted by MD and RS. Experiments for comparison between on-road and test-bed measurements were executed by MD. The work was conducted under academic supervision of CB. The first draft of the manuscript was written by MD and all authors commented on previous versions of the manuscript. All authors read and approved the final manuscript.

Funding Open Access funding enabled and organized by Projekt DEAL. No funds, grants, or other support was received.

Availability of data and material Due to the nature of this research, data and material are not to be shared publicly, so supporting data are not available.

Code availability Due to the nature of this research, code is not to be shared publicly, so it is not available.

Declarations

Conflict of interest The authors have no conflicts of interest to declare that are relevant to the content of this article.

References

1. Council of the European Communities. Council Directive 91/441/EEC of 26 June 1991 amending Directive 70/220/EEC on the approximation of the laws of the Member States relating to measures to be taken against air pollution by emissions from motor vehicles. Official Journal of the European Communities. https://eur-lex.europa.eu/legal-content/EN/TXT/PDF/?uri=CELEX:31991L0441&from=en (1991). Accessed 26 Jun 2020
2. European Commission. Commission regulation (EU) 2016/646 of 20 April 2016 amending Regulation (EC) No 692/2008 as regards emissions from light passenger and commercial vehicles (Euro 6). Official Journal of the European Union. https://eur-lex.europa.eu/legal-content/EN/TXT/PDF/?uri=CELEX:32016R0646&from=EN (2016). Accessed 26 Jun 2020
3. Fathy, H.K., Filipi, Z.S., Hagena, J., Stein, J.L.: Review of hardware-in-the-loop simulation and its prospects in the automotive area. Proc. SPIE (2006). https://doi.org/10.1117/12.667794
4. Feng, T., Yang, L., Gu Q, Hu, Y., Yan, T., Yan, B.: A supervisory control strategy for plug-in hybrid electric vehicles based on energy demand prediction and route preview. IEEE Trans. Veh. Technol. (2015). https://doi.org/10.1109/TVT.2014.2336378
5. Frank, A.A.: Plug-in Hybrid Vehicles for a Sustainable Future. Am. Sci. (2007). https://doi.org/10.1511/2007.64.158
6. Gonder, J., Simpson, A. Measuring and reporting fuel economy of plug-in hybrid electric vehicles. National renewable energy laboratory. https://www.nrel.gov/docs/fy07osti/40377.pdf (2006). Accessed 26 Jun 2020
7. Gulbins, M., Melcher, A., Ziebert, C., Lei, B., Markwirth, T., Haase, J. Parametrisierung von Lithium-Ionen Zellen auf Basis von CIT Messungen. Workshop ASIM/GI-Fachgruppen simulation technischer systeme grundlagen und methoden in Modellbildung und Simulation, Lippstadt. https://www.researchgate.net/publication/299183174_Parametrisierung_von_Lithium-Ionen_Zellen_auf_Basis_von_CIT_Messungen/references (2016). Accessed 26 Jun 2020
8. Heffner, R.R., Kurani, K.S., Turrentine, T.S.: Driving plug-in hybrid electric vehicles: reports from U.S. drivers of hybrid electric vehicles converted to plug-in hybrid vehicles. Transp. Res. Rec. (2009). https://doi.org/10.3141/2139-05
9. Karbowski, D., Kim, N., Rousseau, A. Route-based online energy management of a PHEV and sensitivity to trip prediction. In: 2014 IEEE vehicle power and propulsion conference (VPPC) (2014). https://doi.org/10.1109/vppc.2014.7007126
10. Keil, P., Jossen, A. Aufbau und parametrierung von batteriemodellen. 19. DESIGN&ELEKTRONIK-Entwicklerforum Batterienand Ladekonzepte, Munich. https://mediatum.ub.tum.de/doc/1162416/ (2012)
11. Kromer, M.A., Heywood, J.B. Electric powertrains: opportunities and challenges in the U.S. light-duty vehicle fleet. MIT Energy Initiative. http://energy.mit.edu/wp-content/uploads/2007/05/MIT-LFEE-07-003-RP.pdf (2007). Accessed 26 Jun 2020
12. Kum, D., Peng, H., Bucknor, N.K.: Optimal energy and catalyst temperature management of plug-in hybrid electric vehicles for minimum fuel consumption and tail-pipe emissions. IEEE Trans. Control Syst. Technol. (2013). https://doi.org/10.1109/tcst.2011.2171344
13. Markel, T., Simpson, A. Energy storage systems considerations for grid-charged hybrid electric vehicles. In: 2005 IEEE Vehicle Power and Propulsion Conference, Chicago, IL, 2005, pp. 6 (2005). https://doi.org/10.1109/VPPC.2005.1554581
14. Markel, T., Wipke, K. Modeling grid-connected hybrid electric vehicles using ADVISOR. In: Sixteenth Annual Battery Conference on Applications and Advances. Proceedings of the

Conference (Cat. No.01TH8533), Long Beach, CA, USA, 2001, pp. 23–29 (2001). https://doi.org/10.1109/BCAA.2001.905095
15. Maschmeyer, H. Systematische Bewertung verbrennungsmotorischer Antriebssysteme hinsichtlich ihrer Realfahrtemissionen am Motorenprüfstand. Dissertation, Technische Universität Darmstadt (2017)
16. Raidt, B., Billinger, T.: Fahrzeugnahe, dynamische Versuche am Motorprüfstand. MTZextra (2017). https://doi.org/10.1007/s41490-017-0007-6
17. Salcher, T., Neumann, L., Krämer, G., Herzog, H.G.: Fuel-efficient state of charge control in hybrid electric vehicles. IEEE Veh. Power (2010). https://doi.org/10.1109/VPPC.2010.5729132
18. Schäfer, F., van Basshuysen, R.: Schadstoffreduzierung und Kraftstoffverbrauch von Pkw-Verbrennungsmotoren. Springer, Vienna (1993)
19. Silva, C., Ross, M., Farias, T.: Evaluation of energy consumption, emissions and cost of plug-in hybrid vehicles. Energy Convers. Manag. (2009). https://doi.org/10.1016/j.enconman.2009.03.036
20. Song, Z. Simulative investigation of the energy management on the endurance loads of plug-in hybrid electric powertrains. Master Thesis, Technische Universität München (2019)
21. United Nations Economic Commission for Europe. Global technical regulation on Worldwide harmonized Light vehicles Test Procedure. UNECE. https://www.unece.org/fileadmin/DAM/trans/main/wp29/wp29r-1998agr-rules/ECE-TRANS-180a15e.pdf (2014). Accessed 26 Jun 2020
22. Wehbe, J., Karami, N. Battery equivalent circuits and brief summary of components value determination of lithium ion: a review. In: 2015 Third International Conference on Technological Advances in Electrical, Electronics and Computer Engineering (TAEECE), Beirut, 2015, pp. 45–49 (2015). https://doi.org/10.1109/TAEECE.2015.7113598
23. You, H.W., Bae, J.I., Cho, S.J., Lee, J.M., Kim, S.H.: Analysis of equivalent circuit models in lithium-ion batteries. AIP Adv. doi **10**(1063/1), 5054384 (2018)
24. Zhang, C., Allafi, W., Dinh, Q., Ascencio, P., Marco, J.: Online estimation of battery equivalent circuit model parameters and state of charge using decoupled least squares technique. Energy (2018). https://doi.org/10.1016/j.energy.2017.10.043